Inorganic Chemistry

Article

pubs.acs.org/IC

Effect of the Cooling Rate on Dimerization of $C_{60}^{\bullet-}$ in Fullerene Salt $(DMI^+)_2{\cdot}(C_{60}^{\bullet-}){\cdot}\{Cd(Et_2NCS_2)_2I^-\}$

Dmitri V. Konarev,*[,†] Salavat S. Khasanov,[‡] Akihiro Otsuka,[§] Hideki Yamochi,[§] Gunzi Saito,[⊥] and Rimma N. Lyubovskaya[†]

[†]Institute of Problems of Chemical Physics RAS, Chernogolovka, Moscow region, 142432 Russia

[‡]Institute of Solid State Physics RAS, Chernogolovka, Moscow region, 142432 Russia

[§]Research Center for Low Temperature and Materials Sciences, Kyoto University, Sakyo-ku, Kyoto, 606-8501 Japan

[⊥]Research Institute, Meijo University, 1-501 Shiogamaguchi, Tempaku-ku, Nagoya, 468-8502 Japan

Supporting Information

ABSTRACT: The salt $(DMI^+)_2{\cdot}(C_{60}^{\bullet-}){\cdot}\{Cd(Et_2NCS_2)_2I^-\}$ (**1**) containing fullerene radical anions, the anions of cadmium diethyldithiocarbamate iodide, and *N*,*N*′-dimethylimidazolium cations was obtained. Fullerenes are monomeric in **1** at 250 K and form three-dimensional packing in which each fullerene has nearly tetrahedral surroundings from neighboring fullerenes. Fullerenes with a shorter interfullerene center-to-center distance of 10.031(2) Å form spiral chains arranged along the lattice *c* axis. The convolution consists of four fullerene molecules. Dimerization realized in **1** within the spiral chains below 135 K manifests a strong dependence on the cooling rate. The "frozen" monomeric phase was obtained upon instant quenching of **1**. This phase is stable below 95 K for a long time but slowly converted to the dimeric phase at $T > 95$ K. It exhibits a weak antiferromagnetic interaction of spins below 95 K (the Weiss temperature is −4 K), which results in the splitting of the electron paramagnetic resonance (EPR) signal into two components below 10 K. A disordered phase containing both $C_{60}^{\bullet-}$ monomers and singly bonded $(C_{60}^-)_2$ dimers with approximately 0.5/0.5 occupancies is formed at an intermediate cooling rate (for 20 min). The position of each fullerene in this phase is split into three positions slightly shifted relative to each other. The central position corresponds to nonbonded fullerenes with interfullerene center-to-center distances of 9.94−10.00 Å. Two other positions are coincided to dimeric fullerenes formed with the right and left fullerene neighbors within the spiral chain. This intermediate phase is paramagnetic with nearly zero Weiss temperature due to isolation of $C_{60}^{\bullet-}$ by diamagnetic species and exhibits a strongly asymmetric EPR signal below 20 K. A diamagnetic phase containing ordered singly bonded $(C_{60}^-)_2$ dimers can be obtained only upon slow cooling of the crystal for 6 h.

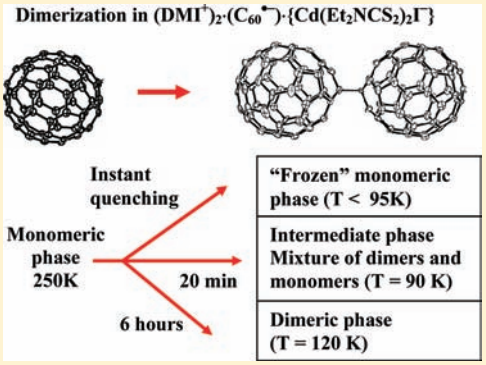

INTRODUCTION

Ionic fullerene compounds show a variety of optical, magnetic, and conducting properties.[1] Negatively charged fullerenes can present in these compounds in monomeric form[2] as well as form dimeric and polymeric structures either in ambient conditions or under small pressure.[3,4] Those are singly[3a−l] and doubly[3m,n] bonded $(C_{60}^-)_2$ dimers and linear $(C_{60}^-)_x$, $(C_{60}^{3-})_x$, and $(C_{70}^{2-})_x$ and two-dimensional $(C_{60}^{4-})_x$ polymers.[4] The study of the formation of singly bonded $(C_{60}^-)_2$ dimers allows one to understand some peculiarities of the formation of different *σ*-bonded structures from negatively charged fullerenes. Some of these structures can manifest interesting magnetic and conducting properties because of preservation of the spins of $C_{60}^{\bullet-}$ even at low temperatures.

To date, the singly bonded $(C_{60}^-)_2$ dimers were found in metastable $M{\cdot}C_{60}$ salts (M = K, Rb, and Cs),[3a,b] ionic compounds $\{Cr(C_6H_5Me)_2\}{\cdot}C_{60}$,[3c] $Cp^*_2Cr{\cdot}C_{60}{\cdot}(C_6H_4Cl_2)_2$,[3d,e] $\{Cr(C_6H_6)_2\}{\cdot}C_{60}{\cdot}C_6H_5CN$,[3e] $\{Cr(C_6H_6)_2\}{\cdot}C_{60}{\cdot}C_6H_4Cl_2$,[3e,f] $Cp_2Co{\cdot}C_{60}{\cdot}C_6H_4Cl_2$,[3e] $\{Cr(C_6H_5{-}C_6H_5)_2\}{\cdot}C_{60}$,[3g] and $(MDABCO)_2{\cdot}(C_{60})_2{\cdot}ET$,[3h] fullerene salts with positively charged gold clusters,[3i] $\{Cr(C_6H_6)_2\}{\cdot}C_{60}{\cdot}[Pd(dbdtc)_2]_{0.5}$,[3j] fullerene salts with tetraphenylporphyrins coordinating nitrogen-containing cations $\{(TMP^+)_2{\cdot}M^{II}TPP\}{\cdot}(C_{60}^-)_2{\cdot}(C_6H_4Cl_2)_2{\cdot}(C_6H_5CN)_2$ (M = Zn and Mn),[3k] and some other compounds[3l] (see abbreviations[5]). The effect of the cooling rate on the formation of *σ*-bonded fullerene structures was found in the $M{\cdot}C_{60}$ salts (M = K, Rb, and Cs) obtained by gas-phase doping of C_{60} with alkali metals.[4a,b] Different fullerene structures were obtained depending on the cooling rate of the high-temperature monomeric phase. Those are stable linear $(C_{60}^-)_x$ polymers[4a,b] and the metastable dimeric phase with singly bonded $(C_{60}^-)_2$ dimers.[3a,b] The "frozen" monomeric phase can be obtained upon instant quenching of the high-temperature monomeric phase to the liquid-nitrogen temperature.[6] The heating of

Received: August 9, 2011
Published: February 29, 2012

   dx.doi.org/10.1021/ic201732t | *Inorg. Chem.* 2012, 51, 3420−3426

$Rb{\cdot}C_{60}$ above 125 K and of $Cs{\cdot}C_{60}$ above 150 K results in dimerization of $C_{60}^{\bullet-}$.[6] Dimerization of $C_{60}^{\bullet-}$ in ionic fullerene compounds is generally observed above 150 K. Hysteresis for such dimerization is small [<2 K for $Cp^*_2Cr{\cdot}C_{60}{\cdot}(C_6H_4Cl_2)_2$[3d,e]], and no noticeable effect of the cooling rate on dimerization was found.[3e] The dimerization temperature is low enough (150−130 K) in $\{Cr(C_6H_6)_2\}{\cdot}C_{60}{\cdot}[Pd(dbdtc)_2]_{0.5}$.[3j] Instant quenching of the compound from room temperature (RT) to 100 K allows one to retain the monomeric phase. However, this phase is unstable at low temperatures and transforms to the dimeric phase below 60 K. The dimeric phase is also formed when this compound is quenched from RT to 4 K.[3j]

We prepare a new fullerene salt, $(DMI^+)_2{\cdot}(C_{60}^{\bullet-}){\cdot}\{Cd(Et_2NCS_2)_2I^-\}$ (**1**), which contains two types of anions and the DMI^+ countercations. Fullerene radical anions are closely packed in **1**, and they are dimerized at low temperatures. The salt manifests the lowest dimerization temperature among studied ionic fullerene compounds (135−120 K). As a result, dimerization strongly depends on the cooling rate. Thus, it is possible to study not only the dimeric phase but also the intermediate phases containing dimers and monomers as well as to suppress dimerization completely. The crystal structure of the high-temperature monomeric phase at 250 K and three crystal structures of the low-temperature phases obtained at different cooling rates are presented. The "frozen" monomeric, intermediate, and ordered dimeric phases were obtained upon instant quenching in a few seconds, a moderate rate of cooling for 20 min, and slower cooling of the sample for 4−6 h, respectively. These phases were characterized by electron paramagnetic resonance (EPR) measurements, which showed different magnetic properties of these phases.

EXPERIMENTAL SECTION

Materials. Sodium ethanethiolate (CH_3CH_2SNa) and hexamethylenetetramine (HMTA) were purchased from Aldrich. C_{60} of 99.98% purity was received from MTR Ltd. Cadmium diethyldithiocarbamate $[Cd(Et_2NCS_2)_2]$[7a] and *N*,*N*′-dimethylimidazolium iodide (DMI·I)[7b] were synthesized according to published procedures. Solvents were purified in an argon atmosphere. *o*-Dichlorobenzene ($C_6H_4Cl_2$) was distilled over CaH_2 under reduced pressure, benzonitrile (C_6H_5CN) was distilled over Na under reduced pressure, and hexane was distilled over sodium/benzophenone. The solvents were degassed and stored in a glovebox. All manipulations for the synthesis of **1** were carried out in a MBraun 150B-G glovebox with a controlled atmosphere and the content of H_2O and O_2 of less than 1 ppm. The crystals were stored in the glovebox and sealed in an anaerobic conditions in 2 mm quartz tubes for EPR measurements under 10^{-5} Torr. KBr pellets for IR and UV−visible−near-IR (NIR) measurements were prepared in the glovebox.

Synthesis. For the preparation of crystals of **1**, C_{60} (25 mg, 0.035 mmol), $Cd(Et_2NCS_2)_2$ (100 mg, 0.24 mmol), HMTA (100 mg, 0.71 mmol), CH_3CH_2SNa (30 mg, 0.36 mmol), and DMI·I (40 mg, 0.18 mmol) were stirred in 16 mL of a $C_6H_4Cl_2/C_6H_5CN$ mixture (14:2) for 2 h at 60 °C. The color of the solution changed from violet to violet-brown. The solution was cooled to RT and filtered. The NIR spectrum of the solution indicated the reduction of C_{60} to a 1− charged state. The solution was filtered in a 50 mL glass tube of 1.8 cm diameter with a ground-glass plug, and 30 mL of hexane was layered over the solution. Standing of the tube for 1 month yields crystals of **1** on the walls of the tube. The solvent was decanted from the crystals, which were washed with hexane to give black octahedra with sizes up to 0.5 × 0.5 × 1 mm (the 60% yield). The composition of the salt was determined by the X-ray diffraction study of a single crystal: $(DMI)_2{\cdot}C_{60}{\cdot}(Cd(Et_2NCS_2)_2I)$ (**1**). Several crystals tested from the synthesis had the same unit cell parameters.

General Procedures. UV−visible−NIR spectra were measured in KBr pellets on a Shimadzu 3100 spectrometer in the 240−2600 nm range. Fourier transform infrared (FT-IR) spectra were measured in KBr pellets with a Perkin-Elmer Series 1000 spectrometer (400−7800 cm^{-1}). EPR spectra were recorded with a JEOL JES-TE 200 X-band ESR spectrometer equipped with a JEOL ES-CT470 cryostat. Instant quenching of a polycrystalline sample of **1** from RT was made down to 4 or 80 K in a few seconds. After cooling, the spectra were measured in heating conditions from 4 or 80 K to RT. Cooling with an intermediate rate was carried out for 20 min. Slow cooling takes about 4 h. To obtain the hysteresis loop, the sample of **1** was measured upon cooling from RT to 80 K for ∼4 h and then from 80 K to RT.

X-RAY CRYSTAL STRUCTURE DETERMINATION

The monomeric phase of **1** was studied at 250 K (**1a**). The "frozen" monomeric phase (**1b**) was obtained upon instant quenching of a single crystal from RT to 95(2) K. It was placed in a nitrogen flow at a temperature of 95(2) K for a few seconds. The dimeric phase was obtained upon slow cooling of the single crystal from RT to 120(2) K for 6 h (**1c**). The intermediate phase was obtained by cooling of the single crystal from RT to 90(2) K for 20 min (**1d**).

Crystal data for **1a** at 250.0(2) K: $C_{80}H_{38}CdN_6S_4I$, M_r = 1450.70 g mol^{-1}, black octahedron, tetragonal, $P4_1$, a = 16.2447(4) Å, b = 16.2447(4) Å, c = 21.5187(9) Å, V = 5678.6(3) $Å^3$, Z = 4, d_{calcd} = 1.697 g cm^{-3}, μ = 1.134 mm^{-1}, $F(000)$ = 2900, $2\theta_{max}$ = 63°, reflections measured 94913, unique reflections 18683, reflections with $I > 2\sigma(I)$ = 13607, parameters refined 1012, restraints 8885, R1 = 0.0482, wR2 = 0.1240, GOF = 1.016, and CCDC 831876.

Crystal data for **1b** at 95.0(1) K: $C_{80}H_{38}CdN_6S_4I$, M_r = 1450.70 g mol^{-1}, black octahedron, tetragonal, $P4_1$, a = 16.1224(3) Å, b = 16.1224(3) Å, c = 21.3629(6) Å, V = 5552.9(2) $Å^3$, Z = 4, d_{calcd} = 1.735 g cm^{-3}, μ = 1.160 mm^{-1}, $F(000)$ = 2900, $2\theta_{max}$ = 63.02°, reflections measured 80348, unique reflections 18404, reflections with $I > 2\sigma(I)$ = 17525, parameters refined 1020, restraints 1042, R1 = 0.0313, wR2 = 0.0748, GOF = 1.021, and CCDC 831878.

Crystal data for **1c** at 120.0(1) K: $C_{80}H_{38}CdN_6S_4I$, M_r = 1450.70 g mol^{-1}, black octahedron, monoclinic, $P112_1$, a = 15.9638(7) Å, b = 16.1658(7) Å, c = 21.4127(7) Å, γ = 90.424(4)°, V = 5525.8(4) $Å^3$, Z = 2, d_{calcd} = 1.744 g cm^{-3}, μ = 1.165 mm^{-1}, $F(000)$ = 2900, $2\theta_{max}$ = 61°, reflections measured 64277, unique reflections 26265, reflections with $I > 2\sigma(I)$ = 21104, parameters refined 1316, restraints 22901, R1 = 0.0713, wR2 = 0.1939, GOF = 1.112, and CCDC 831879.

Crystal data for **1d** at 90.0(3) K: $C_{80}H_{38}CdN_6S_4I$, M_r = 1450.70 g mol^{-1}, black octahedron, tetragonal, $P4_1$, a = 16.0960(3) Å, b = 16.0960(3) Å, c = 21.3845(6) Å, V = 5540.3(2) $Å^3$, Z = 4, d_{calcd} = 1.740 g cm^{-3}, μ = 1.162 mm^{-1}, $F(000)$ = 2904, $2\theta_{max}$ = 61.02°, reflections measured 84767, unique reflections 16879, reflections with $I > 2\sigma(I)$ = 16058, parameters refined 1140, restraints 701, R1 = 0.0358, wR2 = 0.0796, GOF = 1.037, and CCDC 831877.

X-ray diffraction data were collected on an Oxford diffraction Gemini-R CCD diffractometer with graphite-monochromated Mo Kα radiation using an Oxford Instruments Cryojet system. Raw data reduction to F^2 was carried out using *CrysAlisPro*, Oxford Diffraction Ltd. The structures were solved by direct methods and refined by a full-matrix least-squares method against F^2 using *SHELX-97*.[8] Non-hydrogen atoms were refined in the anisotropic approximation. The positions of the hydrogen atoms were calculated geometrically. Subsequently, the positions of the hydrogen atoms were refined by the

dx.doi.org/10.1021/ic201732t | *Inorg. Chem.* 2012, 51, 3420−3426

"riding" model with $U_{iso} = 1.2U_{eq}$ of the connected non-hydrogen atom or as ideal CH_3 groups with $U_{iso} = 1.5U_{eq}$.

To keep the fullerene geometry close to ideal in the disordered groups, bond-length restraints were used along with the next-nearest neighbor distances, using the SADI SHELXL instruction. To keep the anisotropic thermal parameters of the fullerene atoms within reasonable limits, the displacement components were restrained using ISOR and DELU SHELXL instructions. That results in a great number of restraints used for the refinement of the crystal structures of **1a**–**1d**.

Disorder. The DMI^+ cations and $Cd(Et_2NCS_2)_2I^-$ anions are ordered in **1a**–**1d**.

1a [250.0(2) K]. Monomeric $C_{60}^{\bullet-}$ are rotationally disordered between two orientations with 0.601(4)/0.399(4) occupancies.

1b [95.0(1) K]. Monomeric $C_{60}^{\bullet-}$ are rotationally disordered between two orientations with 0.648(2)/0.352(2) occupancies.

Figures 1 and 2 show a major occupied orientation of $C_{60}^{\bullet-}$ only.

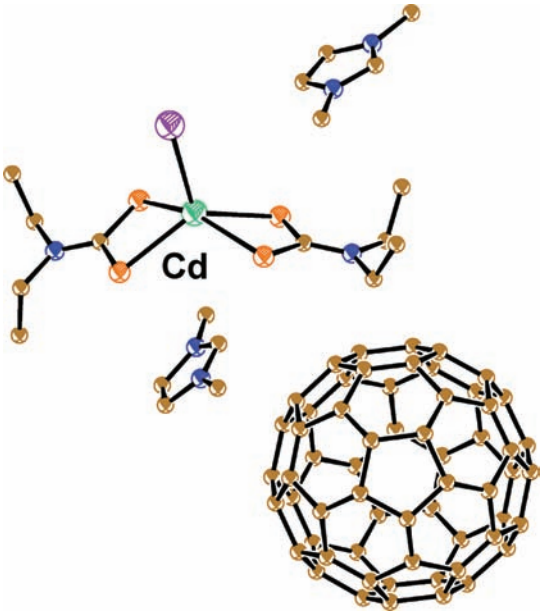

Figure 1. Crystallographically independent unit in the monomeric phase of **1** at 250 K.

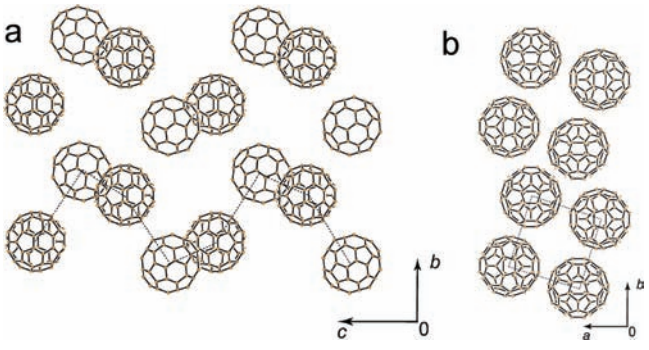

Figure 2. Packing motif of $C_{60}^{\bullet-}$ in the monomeric phase of **1** at 250 K: (a) view along the *a* axis showing two fullerene spiral chains; (b) view along the *c* axis and the fullerene spiral chains. The dashed lines indicate one spiral chain from fullerenes.

1c [120.0(1) K]. All components are well ordered in the slowly cooled dimeric phase.

1d (90.0(3) K). The position of each C_{60} is split into three positions. The central position is occupied by monomeric $C_{60}^{\bullet-}$ [the total occupancy is 0.498(2)]. Fullerene in this position is rotationally disordered between two orientations with 0.266(3)/0.232(3) occupancies. Two other positions are occupied by fullerenes involved in the $(C_{60}^-)_2$ dimers. They are shifted to the right and left sides relative to the central position and have 0.251(2)/0.251(2) occupancies, respectively. The total occupancy of two of these positions is 0.502(2).

RESULTS AND DISCUSSION

a. Synthesis. Previously, we studied molecular compound $[\{Zn(Et_2NCS_2)_2\}\cdot HMTA]_2\cdot C_{60}\cdot C_6H_5Cl$ containing large vacancies.[9] Because solvent can be substituted in some compounds by small cations, we tried to synthesize ionic complex $(C_{60}^{\bullet-})\cdot(DMI^+)\cdot(\{Cd(Et_2NCS_2)_2\}\cdot HMTA)$. In reaction, fullerene was reduced by sodium ethanethiolate (CH_3CH_2SNa) in the presence of the *N*,*N*′-dimethylimidazolium cations (DMI^+), neutral cadmium diethyldithiocarbamate ($Cd(Et_2NCS_2)_2$), and hexamethylenetetramine. However, instead of the formation of $\{Cd(Et_2NCS_2)_2\}\cdot HMTA$, iodine anions originating from the $(DMI^+)\cdot(I^-)$ salt coordinated to neutral $Cd(Et_2NCS_2)_2$ to form an anion with a five-coordinated cadmium atom, $Cd(Et_2NCS_2)_2I^-$. As a result, the compound crystallized contains two different anionic species: $C_{60}^{\bullet-}$ and $Cd(Et_2NCS_2)_2I^-$ (Figure 1). It is noteworthy that the use of HMTA is indispensable to synthesize single crystals because without this ligand the salt quantitatively precipitates for 1 day and high-quality crystals cannot be obtained. Most probably, $Cd(Et_2NCS_2)_2\cdot HMTA$, which forms at the first stage, slowly transforms to the $Cd(Et_2NCS_2)_2I^-$ anions by substitution of HMTA with I^-. This provides slow crystallization of $(DMI^+)_2\cdot(C_{60}^{\bullet-})\cdot(Cd(Et_2NCS_2)_2I^-)$ (**1**) as single crystals. The reaction can be presented by the following scheme:

$$C_{60} + CH_3CH_2S^-Na^+ + Cd(Et_2NCS_2)_2 + (2DMI^+I^-)$$
$$\rightarrow C_{60}^- + Cd(Et_2NCS_2)_2I^- + 2(DMI^+) +$$
$$0.5(CH_3CH_2S)_2 + NaI$$
$$\rightarrow \mathbf{1}\cdot 0.5(CH_3CH_2S)_2 + NaI$$

where sodium ethanethiolate (CH_3CH_2SNa) was used to reduce C_{60}.

b. Spectra of 1 in the IR and Visible–NIR Ranges. The charged state of fullerenes is estimated by spectral methods (Supporting Information). The positions of the absorption bands of C_{60} in the IR spectrum of **1** are at 523, 576, and 1390 cm^{-1}. The last band belongs to the $F_{1u}(4)$ mode, which is most sensitive to the charged state of C_{60} and shifts from 1429 cm^{-1} (the neutral state) to 1386–1396 cm^{-1} (the 1− charged state).[1e,3e,10] The 1− charged state of C_{60} is estimated based on the position of this mode in the spectrum of **1**. The band at 576 cm^{-1} has essentially a higher intensity than that of the band at 523 cm^{-1}. That is also characteristic of fullerene radical anions.[10a] The visible–NIR spectrum of **1** supports the formation of $C_{60}^{\bullet-}$ due to the presence of characteristic bands at 962 and 1078 nm.[1e,3e,10b,c] Additionally, the absorption bands of DMI^+ and $Cd(Et_2NCS_2)_2I^-$ are also observed. The formation of coordination structures of metal(II) dialkyldithiocarbamates with N-containing ligands shifts the

dx.doi.org/10.1021/ic201732t | Inorg. Chem. 2012, 51, 3420–3426

position of their intense bands at 1497−1507 cm^{-1} by 9−17 cm^{-1}.[9] The coordination of the I^- anion to $Cd(Et_2NCS_2)_2$ results in an even stronger shift of the split band of $Cd(Et_2NCS_2)_2$ at 1497 and 1507 cm^{-1} to 1482 cm^{-1} (**1**).

c. Crystal Structure of the Monomeric Phase at 250.0(2) K. The structure of the monomeric phase of **1** was analyzed at 250 K. The salt has a tetragonal lattice with a $P4_1$ space group and three-dimensional (3D) packing of the $C_{60}^{\bullet-}$ radical anions in which each fullerene has nearly tetrahedral surroundings from neighboring fullerenes. Two center-to-center distances are equal to 10.031(2) Å, and two other distances are equal to 10.110(2) Å. Fullerenes with shorter interfullerene center-to-center distances form spiral chains arranged along the lattice *c* axis (Figure 2). Convolution consists of four fullerene anions (Figure 2b). The absolute configuration of the spiral was checked up on the Flack parameter, and $x = 0$ corresponds to the right-handed spiral.

The cadmium atom in the $Cd(Et_2NCS_2)_2I^-$ anion is surrounded by one iodine and four sulfur atoms (Figure 1). Two Cd−S bonds are short (2.56−2.57 Å), whereas two other Cd−S bonds and the Cd−I bond are quite long (2.73−2.78 Å). It was shown that metal(II) diethyldithiocarbamates and their coordinatively bound structures can efficiently pack with the nearly spherical fullerene molecules because of the fact that the dihedral angle between the MS_2CN planes in dithiocarbamates of 143.8−148.9° is close to the angle between two C_{60} hexagons (138.5°). Smaller or greater dihedral angles in the dithiocarbamate molecules result in worthy conditions for $\pi-\pi$ interaction and disorder of the fullerene molecules in the complexes.[7a,9] For the $Cd(Et_2NCS_2)_2(I^-)$ anion, the dihedral angle between the MS_2CN planes is small (134.8°). Moreover, the MS_2CN planes rotate relative to each other by 21.6°. That makes efficient packing of $Cd(Et_2NCS_2)_2I^-$ and $C_{60}^{\bullet-}$ impossible. As a result, fullerene radical cations are surrounded only by the ethyl groups and iodine atoms of $Cd(Et_2NCS_2)_2I^-$ and by the methyl groups of DMI^+. $\pi-\pi$ interaction between the dithiocarbamate and fullerene planes characteristic of neutral fullerene−dithiocarbamate complexes[7a,9] is not observed in **1**. Probably, the additional destabilization factor for the close approach of two anions is repulsion of their negative charges.

d. Dimerization of $C_{60}^{\bullet-}$ in 1 at Different Cooling Rates. Dimerization is realized in the salt below 135 K. However, the structure of the low-temperature phase depends on the cooling rate. Instant quenching of a single crystal of **1** from RT to 95 K completely suppresses dimerization, and the monomeric phase is retained. We call this phase the "frozen" monomeric phase because it can exist below 95 K only. X-ray analysis of the single crystal instantly quenched to 100 K showed that the monomeric phase is also retained at this temperature but slowly transforms to the dimeric phase during the X-ray diffraction experiment. No transformation to the dimeric phase was found at 95 K. The "frozen" monomeric phase at 95 K has the same $P4_1$ space group as the monomeric phase at 250 K. The center-to-center interfullerene distances are decreased in the "frozen" monomeric phase at 95 K. The longer interchain center-to-center distance of 10.110(2) Å (250 K) is shortened to 10.030(2) Å (95 K), whereas the shorter center-to-center distance within the spiral chains is shortened from 10.031(2) Å (250 K) to 9.943(2) (95 K).

An unusual phase is formed when the crystal of **1** was cooled from RT to 90 K for 20 min (intermediate cooling rate). Although only one C_{60}^- is crystallographically unique, structure analysis resulted in the wrong solution when only one position was assumed for the fullerene. The structure included a disordered spiral fullerene "polymer" (Figure 3a) with an

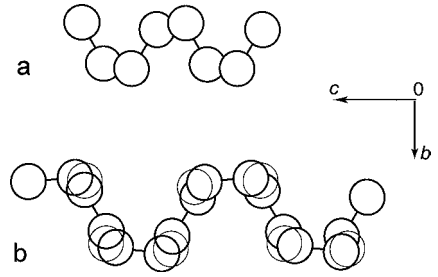

Figure 3. Schematic view of disorder in the intermediate phase: (a) disordered spiral fullerene polymer model in which only one position is assumed for each fullerene site (wrong model); (b) real situation in which the position of the fullerene is split into three positions at each site. Possible dimers formed between the sites are shown by thick circles, and the positions for monomeric C_{60}^- are shown by thin circles.

unusually long interfullerene C−C bond of about 2.2 Å and an interfullerene center-to-center distance of 9.6 Å, which is intermediate between those characteristic of singly bonded $(C_{60}^-)_2$ dimers (9.3 Å)[3a−l] and closely packed monomeric $C_{60}^{\bullet-}$ (9.9 Å).[1c] Careful analysis of fullerene disorder allows one to suppose that the position of fullerene at a site is split into three positions that are slightly shifted relative to each other (Figure 3b). The site occupancy factors (sof's) of the central and other two positions are refined to be 50% and 25%, respectively. The central position corresponds to the non-dimerized monomeric $C_{60}^{\bullet-}$ because the center-to-center distance from this fullerene to the neighboring fullerenes in the central positions are 9.941 Å, the value of which is close to the normal distances between closely packed monomeric $C_{60}^{\bullet-}$.[1c] The intersite center-to-center fullerene distance is 9.3 Å when the nearest positions with 25% sof are considered (Figure 3b). Two atoms in these fullerenes appear to be much more pyramidalized than the others (C301 and C401), indicating the formation of a single bond between fullerenes [the length of this bond is 1.620(4) Å]. The center-to-center distances and length of the intercage C−C bond in these dimers are close to those previously observed for other singly bonded $(C_{60}^-)_2$ dimers.[3a−l] These data indicate that both monomers and dimers coexist in the intermediate phase. It is interesting that previously disordered "polymeric" structures with unusually long interfullerene C−C bonds and center-to-center distances were observed, for example, in $(Cr^I(C_6H_5CH_3)_2^{\bullet+})\cdot(C_{60}^{\bullet-})\cdot CS_2$.[11] The observation of such a "polymer" is possible when dimerization is not complete because of the fast cooling rate, and an intermediate phase containing monomers and dimers is formed. If the position of the fullerene is not split into several positions, this phase looks like a disordered "polymer". The interfullerene C−C bond length and center-to-center interfullerene distance in such a "polymer" depend on a ratio of monomers and dimers and decrease when the content of the dimers increases.

The dimeric phase was obtained upon slow cooling of the crystal from RT to 120 K for 6 h (Figure 4). The symmetry of the unit cell decreases upon dimerization to the monoclinic system with the $P112_1$ space group. Because dimerization of $C_{60}^{\bullet-}$ is realized within spiral chains (Figure 2), the spiral

dx.doi.org/10.1021/ic201732t | Inorg. Chem. 2012, 51, 3420−3426

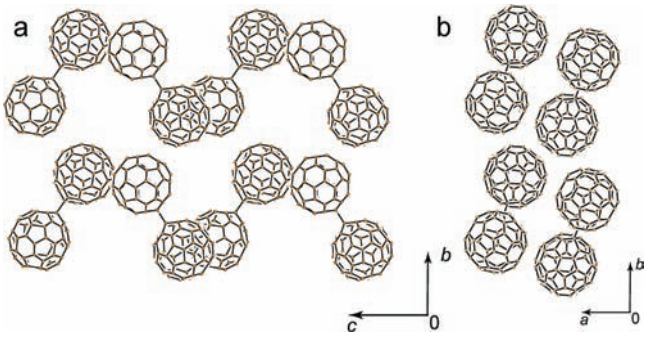

Figure 4. Crystal structure of the ordered dimeric phase at 120 K obtained upon slow cooling of a single crystal: view of two spirals from the $(C_{60}^{-})_2$ dimers along the *a* (a) and *c* axes (b).

arrangement of the $(C_{60}^{-})_2$ dimers is also observed (Figure 4). Spiral chains of dimers are isolated to each other because the center-to-center distances between fullerenes within the spiral chain are short [9.331(4) and 10.041(4) Å], but such distances between fullerenes from neighboring spiral chains increase up to 10.158(4) Å. In contrast to the disordered "intermediate" phase, dimerization at a slow cooling rate affords completely ordered fullerene dimers. Therefore, slow cooling is an important factor in obtaining an ordered dimeric structure at low temperature. The interfullerene C−C bond length and center-to-center distance in the $(C_{60}^{-})_2$ dimers of 1.62(1) and 9.331(4) Å are close enough to those for singly bonded $(C_{60}^{-})_2$ dimers studied previously.[3a−l]

e. Effect of the Cooling Rate on the Magnetic Properties of 1. The magnetic properties of **1** were studied on a polycrystalline sample. The salt manifests a broad EPR signal at RT with g = 2.0021 and a line width (ΔH) of 15 mT. The signal belongs to the $C_{60}^{\bullet-}$ radical anions because both $Cd(Et_2NCS_2)_2I^-$ and DMI^+ species are diamagnetic and EPR-silent. The signal with similar parameters was previously found in $(DMI^+)_3{\cdot}(C_{60}^{\bullet-}){\cdot}(I^-)_2$ salt (g = 2.0035 and ΔH = 21.5 mT at RT).[7b] Therefore, namely, DMI^+ containing fullerene salts show larger g-factor values and broader EPR signals than those observed for ionic C_{60} compounds (g = 1.9996−2.0000 and ΔH = 2−6 mT at RT).[1e,3c,l]

In the slow cooling process of the monomeric phase for 4 h from RT to 80 K, the intensity of the EPR signal showed a distinct decrease at 135−125 K, which corresponds to dimerization of $C_{60}^{\bullet-}$ observed in the structural analyses (Figure 5). That is the lowest dimerization temperature so far observed in the ionic fullerene compounds. Previously, dimerization of $C_{60}^{\bullet-}$ at 150−130 K was observed in $\{Cr(C_6H_6)_2\}{\cdot}C_{60}{\cdot}[Pd(dbdtc)_2]_{0.5}$.[3j] Dimerization in **1** is reversible with hysteresis of about 5 K (Figure 5).

The signal intensity does not decrease upon instant sample quenching from RT down to 90 K (Figure 6). This "frozen" monomeric phase is stable up to 95 K, and an abrupt drop of the signal intensity from $C_{60}^{\bullet-}$ is observed when the sample is heated above 95 K (Figure 6). This decrement of spin susceptibility well corresponds to the previously mentioned transformation to the diamagnetic dimeric phase proven by X-ray diffraction studies. A similar transformation of the "frozen" monomeric phase to the dimeric phase was observed in $M{\cdot}C_{60}$ salts above 125−150 K.[6] For the title salt, dimers formed upon heating above 95 K dissociate only above 125 K, which results in the growth of the intensity of the EPR signal (Figure 6).

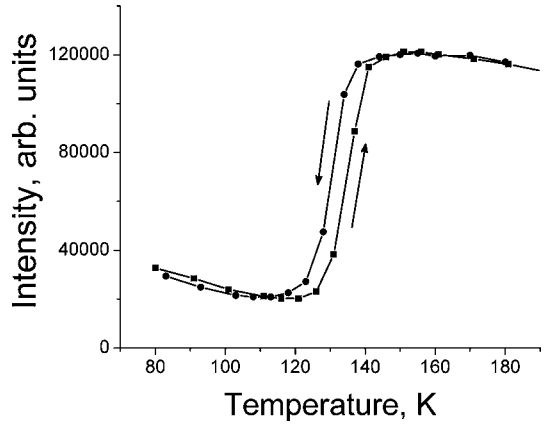

Figure 5. Changes of the integral intensity of the EPR signal from $C_{60}^{\bullet-}$ at the dimerization in **1** upon slow cooling from RT to 80 K (circles) and heating (squares) from 80 K to RT.

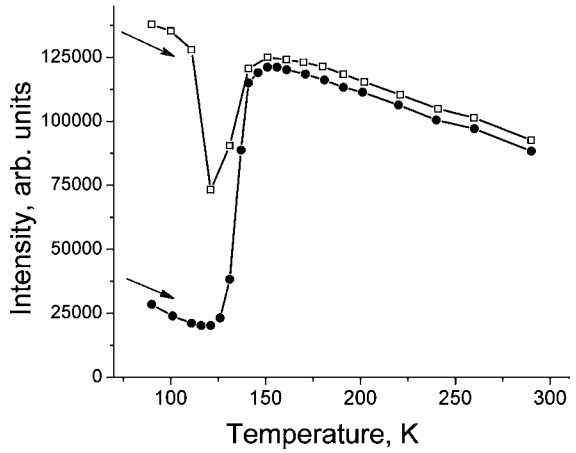

Figure 6. Temperature dependence of the integral intensity of the EPR signal of polycrystalline **1** upon heating the sample prepared by slow cooling (4 h, full circles) and instant quenching (seconds, open squares) from RT to 90 K.

Analysis of the spectra measured at an intermediate cooling rate for 20 min from RT to 90 K shows that dimerization cannot occur completely and about 50% of the $C_{60}^{\bullet-}$ monomers are still present in the sample because the signal intensity at 90 K is intermediate between those observed for instantly quenched and slow-cooled samples of **1**.

f. Magnetic Properties of "Frozen" Monomeric and Intermediate Phases at Low Temperatures (4−95 K). Upon instant quenching of **1** from RT to 4 K, the EPR signal did not lose its intensity. While the intensity was unchanged for 2 h at 4 K showing the stability of this phase, the signal was split into two components at this temperature (Figure 7). The parameters of each component at 6 K are g_1 = 2.0016, ΔH = 0.50 mT and g_2 = 2.0057, ΔH = 0.80 mT. The splitting of the signal from $C_{60}^{\bullet-}$ into two components is generally observed in the ionic fullerene compounds, which manifest weak antiferromagnetic interaction of spins.[12] Indeed, the temperature dependence of the intensity of the EPR signal of **1** at 4−95 K can be well described by the Curie−Weiss law, with a negative Weiss temperature of −4 K indicating weak antiferromagnetic interaction of spins, which can be realized in a 3D packing of fullerenes. A similar antiferromagnetic interaction of spins with the Weiss temperature of −9.6 K was found in

dx.doi.org/10.1021/ic201732t | Inorg. Chem. 2012, 51, 3420−3426

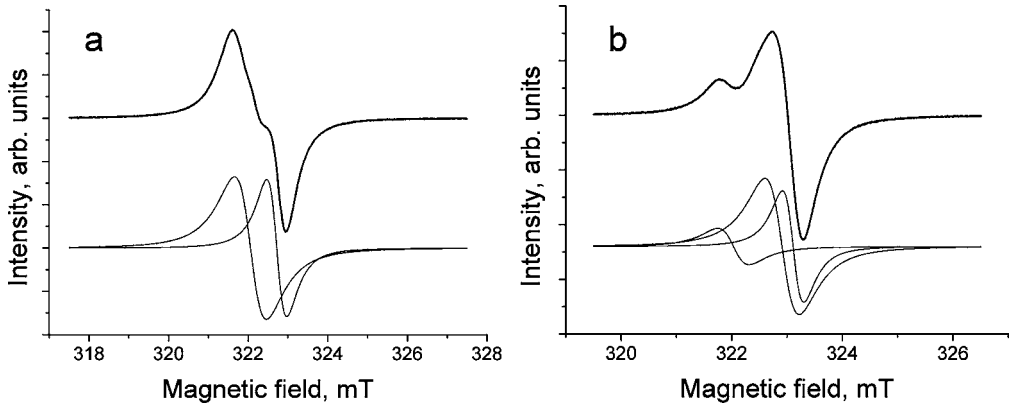

Figure 7. EPR signal of polycrystalline **1** at 6 K: (a) "frozen" monomeric phase obtained upon instant quenching of the sample from RT to 4 K; (b) intermediate phase containing fullerene dimers and monomers. For each, the observed spectrum is shown in top and the deconovolution with Lorentzian shaped signals is depicted in bottom.

$(DMI^+)_3{\cdot}(C_{60}^{\bullet-}){\cdot}(I^-)_2$ with the hexagonal 3D fullerene array.[7b] The EPR signal becomes a single Lorentzian above 10 K. The temperature dependence of the signal integral intensity above 80 K is identical with that for the sample instantly quenched from RT to 80 K. The drop of the intensity of the EPR signal is also observed above 95 K. The g factor of the signal is nearly temperature-independent up to RT, whereas the signal is strongly broadened at $T > 30$ K (Supporting Information).

The intermediate phase shows different magnetic behavior at low temperatures. The signal is strongly asymmetric below 20 K and can be fitted by three components: $g_1 = 2.0012$, $\Delta H = 0.38$ mT; $g_2 = 2.0024$, $\Delta H = 0.62$ mT; $g_3 = 2.0079$, $\Delta H = 0.57$ mT at 6 K (Figure 7b). The signal turns to Lorentzian shape at 20 K, and above this temperature, it has a g factor and a line width similar to those of the signal from the "frozen" monomeric phase. The temperature dependence of the integral intensity of this signal at 4–95 K can be well fitted by the Curie–Weiss expression with nearly zero Weiss temperature. That indicates the absence of noticeable magnetic interaction between monomeric $C_{60}^{\bullet-}$ radical anions in the intermediate phase. The reason for that can be magnetic isolation of the remaining paramagnetic $C_{60}^{\bullet-}$ radical anions by diamagnetic species [the $(C_{60}^-)_2$ dimers, DMI^+ cations, and $Cd(Et_2NCS_2)_2I^-$ anions].

CONCLUSION

We obtained new salt of fullerene **1** with 3D fullerene packing in which spiral chains from $C_{60}^{\bullet-}$ are formed along the lattice c axis. Fullerenes are closely packed in the spiral chains and are dimerized below 135 K. That is the lowest dimerization temperature observed in the ionic fullerene compounds.[3c,l] "Retarded" dimerization results in a hysteretic behavior and a strong dependence of dimerization on the cooling rate. The monomeric phase can be frozen upon instant quenching. It exists for a long time below 95 K and transforms to the more stable dimeric phase above this temperature. This phase exhibits a weak antiferromagnetic interaction of spins. An intermediate cooling rate yields a paramagnetic phase simultaneously containing fullerene dimers and monomers. For this phase, three positions are assumed for each fullerene to obtain the most reliable crystal structure. Judging from the interfullerene center-to-center distance, the central position is occupied by monomeric fullerenes and two other positions are occupied by fullerenes involved in the $(C_{60}^-)_2$ dimers. A diamagnetic ordered dimeric phase was obtained at a slow cooling rate. These data show that monomeric phases can be frozen in some cases upon instant quenching of the samples, and intermediate phases containing dimers and monomers can be obtained. In whole, salt **1** exhibits two interesting features such as a spiral arrangement of fullerene anions in a crystal and cooling-rate-dependent phase-transition behavior.

ASSOCIATED CONTENT

Supporting Information

X-ray crystallographic data in CIF format, IR and UV–visible–NIR spectra, and temperature behavior of the g factor and line width of the EPR signal. This material is available free of charge via the Internet at http://pubs.acs.org.

AUTHOR INFORMATION

Corresponding Author

*E-mail: konarev@icp.ac.ru.

ACKNOWLEDGMENTS

The work was supported by RFBR Grants 09-02-01514 and 12-03-92107 and Grant-in-Aid Scientific Research from JSPS, Japan (Grant 23225005), and MEXT, Japan (Grant 20110006).

REFERENCES

(1) (a) Sariciftci, N. S.; Heeger, A. J. In *Handbook of organic conductive molecules and polymers*; Nalwa, H. S., Ed.; John Wiley and Sons Ltd.: New York, 1997; Vol. *1*, p 414. (b) Gotschy, B. *Fullerene Sci. Technol.* **1996**, *4*, 677. (c) Rosseinsky, M. J. *J. Mater. Chem.* **1995**, *5*, 1497. (d) Konarev, D. V.; Khasanov, S. S.; Otsuka, A.; Maesato, M.; Saito, G.; Lyubovskaya, R. N. *Angew. Chem.* **2010**, *49*, 4829. (e) Konarev, D. V.; Lyubovskaya, R. N. *Russ. Chem. Rev.* **1999**, *68*, 19.

(2) (a) Pènicaud, A.; Hsu, J.; Reed, C. A.; Koch, A.; Khemani, K. C.; Allemand, P.-M.; Wudl, F. *J. Am. Chem. Soc.* **1991**, *113*, 6699. (b) Bhyrappa, P.; Paul, P.; Stinchcombe, J.; Boyd, P. D. W.; Reed, C. A. *J. Am. Chem. Soc.* **1993**, *115*, 11004. (c) Konarev, D. V.; Khasanov, S. S.; Saito, G.; Vorontsov, I. I.; Otsuka, A.; Lyubovskaya, R. N.; Antipin, Yu. M. *Inorg. Chem.* **2003**, *42*, 3706. (d) Paul, P.; Xie, Z.; Bau, R.; Boyd, P. D. W.; Reed, C. A. *J. Am. Chem. Soc.* **1994**, *116*, 4145. (e) Hong, J.; Shores, M. P.; Elliott, C. M. *Inorg. Chem.* **2010**, *49*, 11378. (f) Bele Boeddinghans, M.; Salzinger, M.; Fassler, T. F. *Chem.—Eur. J.* **2009**, 3261. (g) Sun, Y.; Reed, C. A. *J. Chem. Soc., Chem. Commun.* **1997**, 747.

(3) (a) Zhu, Q.; Cox, D. E.; Fischer, J. E. *Phys. Rev. B* **1995**, *51*, 3966. (b) Oszlányi, G.; Bortel, G.; Faigel, G.; Tegze, M.; Grárásy, L.; Pekker, S.; Stephens, P. W.; Bendele, G.; Dinnebier, R.; Mihály, G.; Jánossy,

A.; Chauvet, O.; Forró, L. *Phys. Rev. B* **1995**, *51*, 12228. (c) Hönnerscheid, A.; Wüllen, L.; Jansen, M.; Rahmer, J.; Mehring, M. *J. Chem. Phys.* **2001**, *115*, 7161. (d) Konarev, D. V.; Khasanov, S. S.; Otsuka, A.; Saito, G. *J. Am. Chem. Soc.* **2002**, *124*, 8520. (e) Konarev, D. V.; Khasanov, S. S.; Saito, G.; Otsuka, A.; Yoshida, Y.; Lyubovskaya, R. N. *J. Am. Chem. Soc.* **2003**, *125*, 10074. (f) Konarev, D. V.; Khasanov, S. S.; Kovalevsky, A. Yu.; Saito, G.; Otsuka, A.; Lyubovskaya, R. N. *Dalton Trans.* **2006**, 3716. (g) Ketkov, S. Yu.; Domrachev, G. A.; Obèdkov, A. M.; Vasìlkov, A. Yu.; Yurèva, L. P.; Mehner, C. P. *Russ. Chem. Bull.* **2004**, *53*, 1932. (h) Konarev, D. V.; Khasanov, S. S.; Saito, G.; Otsuka, A.; Lyubovskaya, R. N. *J. Mater. Chem.* **2007**, *17*, 4171. (i) Schulz-Dobrick, M.; Jansen, M. *Angew. Chem., Int. Ed.* **2008**, *47*, 2256. (j) Konarev, D. V.; Kovalevsky, A. Yu.; Otsuka, A.; Saito, G.; Lyubovskaya, R. N. *Inorg. Chem.* **2005**, *44*, 9547. (k) Konarev, D. V.; Khasanov, S. S.; Mukhamadieva, G. R.; Zorina, L. V.; Otsuka, A.; Yamochi, H.; Lyubovskaya, R. N. *Inorg. Chem.* **2010**, *49*, 3881. (l) Konarev, D. V.; Khasanov, S. S.; Lyubovskaya, R. N. *Russ. Chem. Bull.* **2007**, *56*, 371. (m) Konarev, D. V.; Khasanov, S. S.; Otsuka, A.; Saito, G.; Lyubovskaya, R. N. *J. Am. Chem. Soc.* **2006**, *128*, 9292. (n) Konarev, D. V.; Khasanov, S. S.; Otsuka, A.; Yamochi, H.; Saito, G.; Lyubovskaya, R. N. *New J. Chem.* **2011**, *35*, 1829.

(4) (a) Stephens, P. W.; Bortel, G.; Faigel, G.; Tegze, M.; Jánossy, A.; Pekker, S.; Oszlanyi, G.; Forró, L. *Nature* **1994**, *370*, 636. (b) Bommeli, F.; Degiory, L.; Wacher, P.; Legeza, O.; Janossy, A.; Oszlanyi, G.; Chauet, O.; Forró, L. *Phys. Rev. B* **1995**, *51*, 14794. (c) Bendele, G.; Stephens, P.; Prassides, K.; Vavekis, K.; Kortados, K.; Tanigaki, K. *Phys. Rev. Lett.* **1998**, *80*, 736. (d) Margadonna, S.; Prassides, K.; Knudsen, K.; Hanfland, M.; Kosaka, M.; Tanigaki, K. *Chem. Mater.* **1999**, *11*, 2960. (e) Brumm, H.; Peter, E.; Jansen, M. *Angew. Chem., Int. Ed.* **2001**, *40*, 2070. (f) Wedig, U.; Brumm, H.; Jansen, M. *Chem.—Eur. J.* **2002**, *8*, 2769. (g) Panthöfer, M.; Wedig, U.; Brumm, H.; Jansen, M. *Solid State Sci.* **2004**, *6*, 619. (h) Oszlányi, G.; Baumgarther, G.; Faigel, G.; Forró, L. *Phys. Rev. Lett.* **1997**, *78*, 4438.

(5) $Cr(C_6H_5Me)_2$: bis(toluene)chromium. Cp^*_2Cr: decamethylchromocene. $Cr(C_6H_6)_2$: bis(benzene)chromium. Cp_2Co: cobaltocene. $Pd(dbdtc)_2$: palladium(II) dibenzyldithiocarbamate. $Cr(C_6H_5\text{-}C_6H_5)_2$: bis(diphenyl)chromium. ET: bis(ethylenedithio)tetrathiafulvalene. $MDABCO^+$: *N*-methyldiazabicyclooctane cation. DMI^+: *N*,*N*′-dimethylimidazolium cation. TMP^+: *N*,*N*′,*N*′-trimethylpiperazinium cation.

(6) Kosaka, M.; Tanigaki, K.; Tanaka, T.; Atake, T.; Lappas, A.; Prassides, K. *Phys. Rev. B* **1995**, *51*, 12018.

(7) (a) Konarev, D. V.; Kovalevsky, A. Yu.; Khasanov, S. S.; Saito, G.; Lopatin, D. V.; Umrikhin, A. V.; Otsuka, A.; Lyubovskaya, R. N. *Eur. J. Inorg. Chem.* **2006**, 1881. (b) Konarev, D. V.; Khasanov, S. S.; Otsuka, A.; Saito, G.; Lyubovskaya, R. N. *CrystEngComm* **2009**, *11*, 811.

(8) Sheldrick, G. M. *Acta Crystallogr., Sect. A* **2008**, *64*, 112.

(9) (a) Konarev, D. V.; Khasanov, S. S.; Lopatin, D. V.; Rodaev, V. I.; Lyubovskaya, R. N. *Russ. Chem. Bull.* **2007**, *56*, 2145. (b) Konarev, D. V.; Kovalevsky, A. Yu.; Khasanov, S. S.; Lopatin, D. V.; Umrikhin, A. V.; Saito, G.; Náfrádi, B.; Forró, L.; Lyubovskaya, R. N. *Cryst. Growth Des.* **2008**, *8*, 1161.

(10) (a) Picher, T.; Winkler, R.; Kuzmany, H. *Phys. Rev. B* **1994**, *49*, 15879. (b) Semkin, N. V.; Spitsina, N. G.; Krol, S.; Graja, A. *Chem. Phys. Lett.* **1996**, *256*, 616. (c) Reed, C. A.; Bolskar, R. D. *Chem. Rev.* **2000**, *100*, 1075.

(11) Broderick, W. E.; Choi, K. W.; Wan, W. C. *Electrochem. Soc. Proc.* **1997**, *14*, 1102.

(12) (a) Konarev, D. V.; Kovalevsky, A. Y.; Khasanov, S. S.; Saito, G.; Otsuka, A.; Lyubovskaya, R. N. *Eur. J. Inorg. Chem.* **2005**, 4822. (b) Konarev, D. V.; Khasanov, S. S.; Otsuka, A.; Saito, G.; Lyubovskaya, R. N. *Inorg. Chem.* **2007**, *46*, 2261. (c) Konarev, D. V.; Khasanov, S. S.; Slovokhotov, Yu. L.; Saito, G.; Lyubovskaya, R. N. *CrystEngComm* **2008**, *10*, 48.